

Digital PLLs for phase noise channels: a concept based on the Tikhonov distribution

*Original*

Digital PLLs for phase noise channels: a concept based on the Tikhonov distribution / Ripani, Barbara; Modenini, Andrea; Montorsi, Guido. - In: IEEE SIGNAL PROCESSING LETTERS. - ISSN 1070-9908. - STAMPA. - 31:(2024), pp. 2040-2044. [10.1109/LSP.2024.3432048]

*Availability:*

This version is available at: 11583/2991001 since: 2024-07-24T07:01:47Z

*Publisher:*

IEEE

*Published*

DOI:10.1109/LSP.2024.3432048

*Terms of use:*

This article is made available under terms and conditions as specified in the corresponding bibliographic description in the repository

*Publisher copyright*

IEEE postprint/Author's Accepted Manuscript

©2024 IEEE. Personal use of this material is permitted. Permission from IEEE must be obtained for all other uses, in any current or future media, including reprinting/republishing this material for advertising or promotional purposes, creating new collecting works, for resale or lists, or reuse of any copyrighted component of this work in other works.

(Article begins on next page)

# Digital PLLs for phase noise channels: a concept based on the Tikhonov distribution

Barbara Ripani<sup>1</sup>, Student Member, IEEE, Andrea Modenini<sup>2</sup>, Guido Montorsi<sup>1</sup> Fellow, IEEE

**Abstract**—We explore the concept of a digital phase-locked loop (PLL) of the first type, derived as an alternative solution to Kalman’s estimation problem by employing the Tikhonov distribution rather than the traditional Gaussian model.

The resulting Tikhonov PLL is a complex-valued nonlinear filter that is simple to implement and demonstrates interesting features in channels affected by strong phase noise. We present a comparative analysis including the classical PLL and Kalman filter to highlight the strengths of the Tikhonov PLL in such contexts.

## I. INTRODUCTION

Current literature on advanced algorithms for phase noise (PN) channels mainly considers two approaches. The first involves advanced demodulation and decoding algorithms (see [1] and reference therein), while the second involves proper shaping of the constellation (e.g., [2], [3]). Focusing on the first approach, the work in [4] derived forward & backward algorithms that are suitable for iterative decoding. In particular, it was found that using the Tikhonov probability distribution function (pdf) to model phase noise probabilities closely matches the actual distributions.

Several variations have been introduced to improve the similarity between the Tikhonov distribution and the actual probabilities. This has been achieved in more challenging scenarios, such as those with the absence of pilots and larger PN variance, by minimizing the Kullback–Leibler divergence or by using expectation propagation [5], [6].

In some applications, the use of forward & backward algorithms, as well as iterative decoding, may not be possible due to engineering constraints such as limited memory and complexity. In many communication systems, carrier synchronization is achieved through the use of PLLs, which are simple and well-established loops that perform their task efficiently under benign conditions. However, when the channel is affected by strong PN, PLLs may fail to properly track the carrier, thus decreasing the signal reception quality.

For this reason, we investigate a possible improvement in PLL performance for PN channels. Since PLLs are a solution to Kalman’s estimation problem [7] where hidden Markov chain variables are Gaussian distributed, we explore how a Tikhonov distribution can be used to derive a new family

Barbara Ripani and Guido Montorsi are with Politecnico di Torino, Department of Electronics and Telecommunications (DET), I-10129 Torino, Italy (email: barbara.ripani@polito.it). Andrea Modenini is with the European Space Agency at European Space Research and Technology Centre (ESA/ESTEC), 2201AZ Noordwijk, The Netherlands (email: andrea.modenini@esa.int). The views expressed herein can in no way be taken to reflect the official opinion of the European Space Agency.

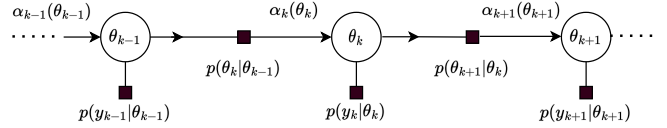


Fig. 1. Factor graph corresponding to (2).

of first-type PLLs that are well-suited for PN channels. The analogy between Tikhonov-based phase estimators and PLL was for the first time recognized by the authors in [5], although they did not delve into the specific technical aspects, as it was beyond the scope of their work. The objective of this letter is therefore to present a Tikhonov-based variation of the classical PLL and analyze its similarities and differences with both Kalman filter (KF) and traditional PLL schemes.

## II. KALMAN FILTER AND PLLS: A FACTOR GRAPH PERSPECTIVE

Consider a pure carrier tone on the Wiener PN channel that, despite its simplicity, is still representative of actual oscillators [8]. The samples of the received signal normalized and in complex base-band are defined as

$$y_k = e^{j\theta_k} + w_k, \quad (1)$$

where  $w_k$  is AWGN with variance  $\sigma^2 = N_0/2PT$  per component,  $N_0$  is the noise power spectral density,  $P$  is the carrier power,  $T$  is the sampling time, and  $\theta_k$  is the  $k$ -th PN sample. The PN process is a random walk, for which

$$\theta_k - \theta_{k-1} \sim \mathcal{N}(\theta_k - \theta_{k-1}, 0, \sigma_\Delta^2),$$

where  $\mathcal{N}(\theta, \mu, \sigma^2)$  indicates a Gaussian distribution in  $\theta$  with mean  $\mu$  and variance  $\sigma^2$ .

Defining the vector  $\mathbf{y}_k = \{y_0, \dots, y_k\}$ , we want to compute the minimum mean square error (MSE) Bayesian estimator  $\hat{\theta}_k = \text{E}[\theta_k|\mathbf{y}_k]$ . This requires the pdf  $p(\theta_k|\mathbf{y}_k)$  that can be derived using the *factor graphs* (FGs) and *sum-product algorithm* (SPA) [9]. Given the vectors  $\boldsymbol{\theta}$  and  $\mathbf{y}$  containing all samples of the phase and received signal, the posterior probability factorizes as

$$p(\boldsymbol{\theta}|\mathbf{y}) \propto p(\theta_0) \prod_{k \geq 0} p(y_k|\theta_k) \prod_{k \geq 1} p(\theta_k|\theta_{k-1}), \quad (2)$$

represented by the FG in Fig. 1. Assuming a symmetrical and non-skewed distribution for the forward messages  $\alpha_k(\theta_k)$ , the MSE estimator can be derived using the SPA as

$$\hat{\theta}_k = \arg \max_{\theta_k} \alpha_k(\theta_k) p(y_k|\theta_k), \quad (3)$$

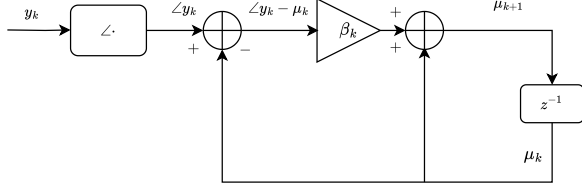


Fig. 2. Block diagrams of the digital PLL.

where  $\forall k$   $\alpha_k(\theta)$  can be recursively computed as

$$\alpha_k(\theta_k) \propto \int_0^{2\pi} \alpha_{k-1}(\theta_{k-1}) p(y_{k-1}|\theta_{k-1}) p(\theta_k|\theta_{k-1}) d\theta_{k-1}. \quad (4)$$

Clearly, it is not possible to solve (3) and (4) in a closed form. However, approximating the messages with distributions belonging to the exponential family, a closed-form solution can be found. For instance, the well-known KF is derived using the Gaussian distribution. Modeling  $p(y_k|\theta_k)$  as  $\mathcal{N}(\theta_k, \angle y_k, \sigma^2)$  and  $\alpha_k(\theta_k)$  as  $\mathcal{N}(\theta_k, \mu_k, \sigma_k^2)$ , the recursion in (4) generates a sequence of Gaussian pdfs. Their mean value and variance can be recursively computed as

$$\mu_{k+1} = \mu_k + \beta_k (\angle y_k - \mu_k) \quad (5)$$

$$\sigma_{k+1}^2 = \frac{1}{(1/\sigma_k^2 + 1/\sigma^2)} + \sigma_\Delta^2, \quad (6)$$

where  $\beta_k$  is known as the *Kalman gain* [10] and is defined as

$$\beta_k = \frac{\sigma_k^2}{\sigma_k^2 + \sigma^2}. \quad (7)$$

Thus, the MSE estimator in (3) is found as

$$\hat{\theta}_k = \mu_{k+1}, \quad (8)$$

and can be implemented using the digital filtering scheme in Fig. 2. In the figure, the phase estimate  $\hat{\theta}_k = \mu_{k+1}$  is updated based on the phase error  $\angle y_k - \mu_k$ . In the recursive calculations in (5) and (6), we can identify the *time-update equations*<sup>1</sup> [10].

The KF steady-state variance satisfies its Riccati equation [11], i.e.  $\sigma_k^2 \rightarrow \sigma_\infty^2$  as  $k \rightarrow \infty$ . As a result, the gain of the KF tends to a steady-state fixed value (denoted as  $\beta_\infty$  as  $k \rightarrow \infty$ ). Substituting (8) into (5), we find

$$\hat{\theta}_k = \hat{\theta}_{k-1} + \beta_\infty (\angle y_k - \hat{\theta}_{k-1}), \quad (9)$$

where one can recognize the equation of a digital PLL of the first type [12] having loop gain  $\beta_\infty$ .

More generally, it can be shown that performing the SPA on the FG in Fig. 1 using an  $N$ -th order Gaussian distribution leads to a KF [9]. In steady-state conditions, when  $N \leq 3$ , this KF becomes equivalent to a PLL of the  $N$ -th type [13]. However, there is a significant difference in the way the two schemes operate. In the standard PLL, the observable

<sup>1</sup>According to the classical Kalman filtering notation [7],  $\mu_k$  represents both the updated state estimation ( $\hat{x}_{k|k}$ ) and the predicted state ( $\hat{x}_{k|k-1}$ ). On the other hand,  $\sigma_k^2$  corresponds to the variance associated with the predicted state ( $\sigma_{k|k-1}^2$ ), while the variance of the update state estimation ( $\sigma_{k|k}^2$ ) is represented by the term  $(1/\sigma_k^2 + 1/\sigma^2)^{-1}$  in (6).

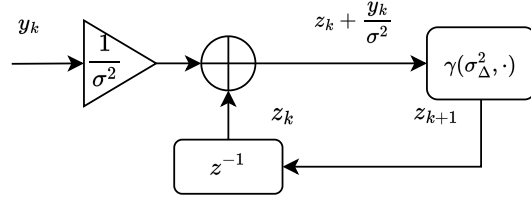


Fig. 3. Block diagram of the digital PLL based on the Tikhonov distribution.

$y_k e^{-j\hat{\theta}_{k-1}}$  is used for carrier tracking [12]. On the other hand, KF uses the most current estimate  $\hat{\theta}_k = \mu_{k+1}$  to directly compensate the signal. Thus, the PLL effectively operates like a KF that provides MSE delayed by one sample, resulting in reduced tracking performance.

### III. TIKHONOV BAYESIAN ESTIMATOR AND PLL

In Section II, we defined the well-known concept of Kalman-PLL duality (see [14], [15]) from the perspective of FGs. In this section, we introduce a new, generalizable model of PLL. We consider using the Tikhonov distribution, another well-known example of the exponential family, to describe the messages flowing along the FG in Fig. 1. We model  $\alpha_k(\theta_k)$  as a circular distribution in  $\theta_k \in [0, 2\pi)$  that reads

$$t(z_k; \theta_k) \propto e^{\Re[z_k e^{-j\theta_k}]},$$

where  $z_k$  is a complex-value parameter. Its angle  $\angle z_k$  determines the mode of the pdf, while  $1/|z_k|$  represents its dispersion. On the other hand,  $p(y_k|\theta_k)$  is by definition  $t(\frac{y_k}{\sigma^2}; \theta_k)$ .

The work in [4] demonstrated that the recursion in (4) can be approximated as a sequence of Tikhonov pdfs with  $z_k$  recursively computed as

$$z_{k+1} = \gamma\left(\sigma_\Delta^2, z_k + \frac{y_k}{\sigma^2}\right), \quad (10)$$

where  $\gamma(x_1, x_2) = \frac{x_2}{1+x_1|x_2|}$ . Thus, the MSE is found to be

$$\begin{aligned} \hat{\theta}_k &= \angle(z_k + y_k/\sigma^2) \\ &= \angle z_{k+1}. \end{aligned} \quad (11)$$

Such an estimator can be implemented with the digital filtering scheme in Fig. 3.

To better understand the behavior of the phase transition in (11), Fig. 4 provides a vector representation of the equation. Consider the scenario in Fig. 4a, where the magnitude of the channel coefficient  $y_k/\sigma^2$  is greater than the forward coefficient  $z_k$ . This situation usually occurs in high signal-to-noise ratio (SNR) scenarios, where the past estimate is less reliable than the channel information. In these cases, the phase estimation, represented by the argument of  $z_k + y_k/\sigma^2$  (equal to that of  $z_{k+1}$ ), tends to closely follow the error identified as  $\angle y_k - \hat{\theta}_{k-1}$ . However, in situations where the magnitude of the forward coefficient dominates over that of the channel term, such as in the scenario depicted in Fig. 4b, the predicted phase will be heavily influenced by the past estimations. This is because the past estimations are more reliable than the channel information.

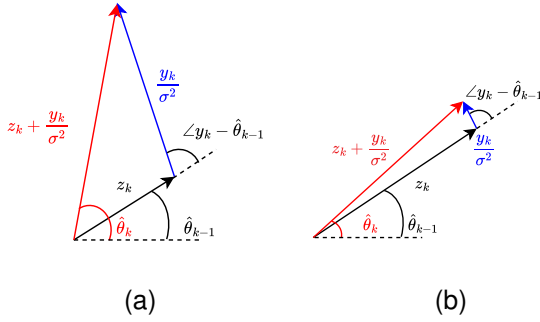


Fig. 4. Vector representation of (11).

We will now prove that the MSE derived in (11) has an equivalency to first-type PLLs, as shown for Kalman filtering. By expanding the terms in (11), we obtain

$$\hat{\theta}_k = \angle \left( |z_k| e^{j\hat{\theta}_{k-1}} + \frac{|y_k|}{\sigma^2} e^{j\angle y_k} \right) \quad (12)$$

$$= \hat{\theta}_{k-1} + \angle \left( |z_k| + \frac{|y_k|}{\sigma^2} e^{j(\angle y_k - \hat{\theta}_{k-1})} \right) \quad (13)$$

$$\approx \hat{\theta}_{k-1} + \frac{|y_k|/\sigma^2}{|z_k| + |y_k|/\sigma^2} (\angle y_k - \hat{\theta}_{k-1}) \quad (14)$$

$$\approx \hat{\theta}_{k-1} + \beta_k (\angle y_k - \hat{\theta}_{k-1}), \quad (15)$$

where (14) was derived by using a linear approximation of the angle (ratio of imaginary and real part) and assuming that the difference  $\angle y_k - \hat{\theta}_{k-1}$  is small. Finally, in (15), we redefine, with an abuse of notation,  $\beta_k$  as

$$\beta_k = \frac{1/|z_k|}{1/|z_k| + \sigma^2/|y_k|}. \quad (16)$$

A preliminary comparison of (15) and (9) reveals the similarity between the two estimators. This similarity is expected in scenarios characterized by reliable estimation, such as those with high SNR. In such contexts, the Tikhonov distribution, characterized by its small dispersion, closely approximates a Gaussian distribution [16]. Consequently, the Tikhonov can be viewed as a Gaussian with variance  $1/|z_k|$ . However, when comparing (7) with (16), we observe the introduction of time dependence on the variance of the measurement ( $\sigma_k^2/|y_k|$ ). Although not demonstrated here, numerical results showed that the gain in (16) does not converge to a steady-state value, but its average  $\mathbb{E}[\beta_k]$  does. Additionally, for high SNR, it holds that  $\mathbb{E}[\beta_k] \rightarrow \beta_\infty$ , and  $1/|z_k| \rightarrow \sigma_\infty^2$ . Thus, despite the fluctuations of  $\beta_k$  in (16) around its mean value, the scheme presented in Fig. 3 introduces a new concept of a first-type digital PLL.

#### IV. KEY ALGORITHMIC FEATURES

In high SNR scenarios, mathematical derivations from Sections II and III suggest that the Kalman and Tikhonov PLLs offer comparable performance. However, having support within the range  $(0, 2\pi]$ , the Tikhonov pdf aligns perfectly with the nature of phase distributions. This results in slightly improved phase estimation in scenarios with strong PN and has implications in scenarios where data modulate the transmitted

carrier. For instance, consider the case of a binary modulation that directly modulates the carrier in (1) with symbols  $x_k \in \{\pm 1\}$ . For demodulation, it is beneficial to perform a “hard” decision on the phase for the KF by compensating the received signal using its estimation. Log-likelihood ratios (LLRs) are then computed, by definition, as

$$\lambda_k = \log \left[ \frac{p(\tilde{y}_k | x_k = 1)}{p(\tilde{y}_k | x_k = -1)} \right],$$

where  $\tilde{y}_k = y_k e^{-j\hat{\theta}_k}$ , and the distribution  $p(\tilde{y}_k | x_k = \pm 1) \sim \mathcal{N}(\tilde{y}_k, x_k = \pm 1, \sigma^2)$ . In contrast, the Tikhonov PLL performs a “soft” approach as described in [4], computing LLRs as

$$\lambda_k = \log \left[ \frac{I_0 \left( \left| z_k + \frac{y_k}{\sigma^2} \right| \right)}{I_0 \left( \left| z_k - \frac{y_k}{\sigma^2} \right| \right)} \right],$$

where  $I_0(\cdot)$  is the modified Bessel function of the first kind and order 0. Section V will show that the Tikhonov-based “soft” approach yields better code-error-rate (CER) performance than the Kalman method. However, it would be possible to explore a hybrid approach that integrates the Kalman phase recursion based on Gaussian distributions with the LLR computation using the soft Tikhonov approach.

#### V. NUMERICAL RESULTS

This section compares the performance of the PLL architectures discussed earlier. These include the classical (first-type) PLL, the KF, the Tikhonov PLL (TK-PLL), and a delayed KF. The latter corresponds to the KF producing a phase estimate with a one-sample delay. As discussed in Section II, the delayed KF represents the maximum performance achievable by classical PLLs, which have a fixed gain that needs to be tuned depending on the scenario.

Consider the case of a pure carrier transmission through a channel affected by PN as in (1). Fig. 5 compares the phase jitter over  $PT/N_0$  for a channel affected by PN with a standard deviation of  $\sigma_\Delta$  of 0.1 and 6 deg. Multiple curves corresponding to different loop gain values for the classical PLL are included in the figure. When  $\sigma_\Delta = 6$  deg, the figure reveals that the TK-PLL outperforms classical PLLs, which are in turn lower-bounded by the KF delayed by one sample. Both the KF and the TK-PLL exhibit a linear decrease in jitter as  $PT/N_0$  increases, with the TK-PLL showing slightly lower jitter at low SNR. When  $\sigma_\Delta$  is small, the jitter of the TK-PLL and the delayed version of the KF coincide, except for low SNR values.

Fig. 6 shows the time-evolution of both the KF gain,  $\beta_k$ , and the TK-PLL mean value,  $\mathbb{E}[\beta_k]$ , with a PN of  $\sigma_\Delta = 6$  deg and  $PT/N_0$  values of 0 and 10 dB. As expected, the KF gain  $\beta_k$  rapidly converges to its steady-state value  $\beta_\infty$ . On the other hand, as discussed in Section III,  $\mathbb{E}[\beta_k]$  tends to  $\beta_\infty$  only in high-SNR scenarios. This can be observed at a  $PT/N_0$  of 10 dB in Fig. 6. However, when  $PT/N_0$  decreases to 0 dB,  $\mathbb{E}[\beta_k]$  converges to a larger value than the Kalman steady-state gain  $\beta_\infty$ . This suggests that, on average, the TK-PLL tends to keep a larger loop bandwidth for more effective PN tracking.

Finally, we consider the transmission of a carrier modulated by binary data as discussed in the previous section. We adopt

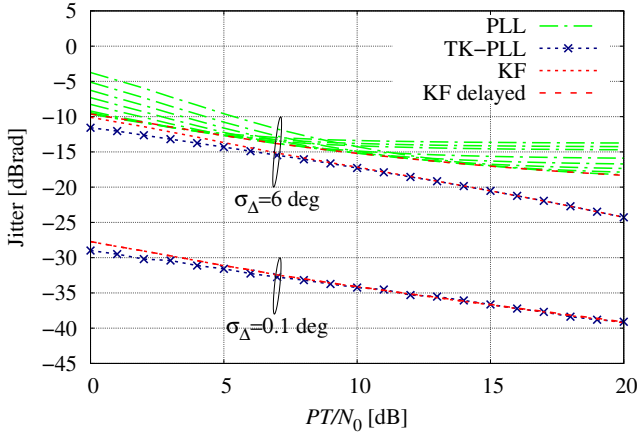


Fig. 5. Jitter performance comparison with PN  $\sigma_{\Delta}$  of 0.1 and 6 deg.

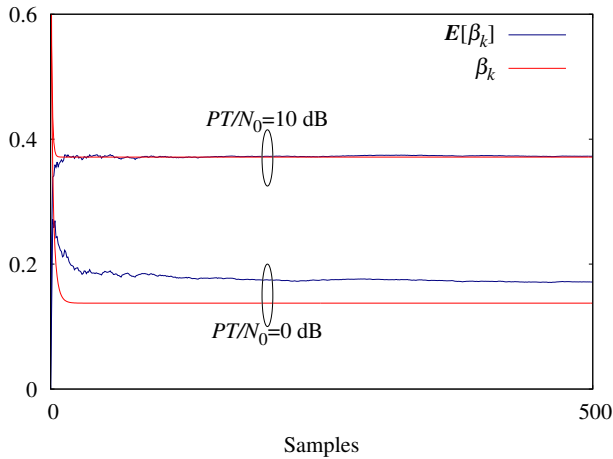


Fig. 6. Evolution of the loop gain  $\beta_k$  (KF) and  $\mathbb{E}[\beta_k]$  (TK-PLL) as function of time, with PN  $\sigma_{\Delta} = 6$  deg, for a  $PT/N_0$  of 0 and 10 dB.

a short low-density parity-check (LDPC) code having a code rate of 1/2 and a block length of 256 [18], as well as binary-shift keying (BPSK) modulation, which is typical of low-rate applications where severe PN may occur. To facilitate the demodulation and tracking, we distribute pilots along the transmitted sequence, with a frequency of one pilot every 20 symbols. Both the KF and the TK-PLL adopt a data-aided approach where an update in the phase estimate only occurs in the presence of pilots. Fig. 7 compares the CER of the two schemes when the phase noise process has standard deviation  $\sigma_{\Delta}$  of 1.5 and 6 deg. As the figure shows, the performance of the TK-PLL and the KF algorithms is nearly identical for a small phase noise of  $\sigma_{\Delta}$  of 1.5 deg. However, the TK-PLL algorithm performs better with a higher value of PN standard deviation (6 deg). The results in Figures 5 and 6 revealed identical phase tracking capabilities for both algorithms. Hence, the disparity in CER between the two algorithms under  $\sigma_{\Delta} = 6$  deg can be attributed to differences in their LLR computation. For small values of  $\sigma_{\Delta}$ ,  $I_0(\cdot)$  behaves similarly to an exponential function. This explains the minimal differences observed between the two CER curves

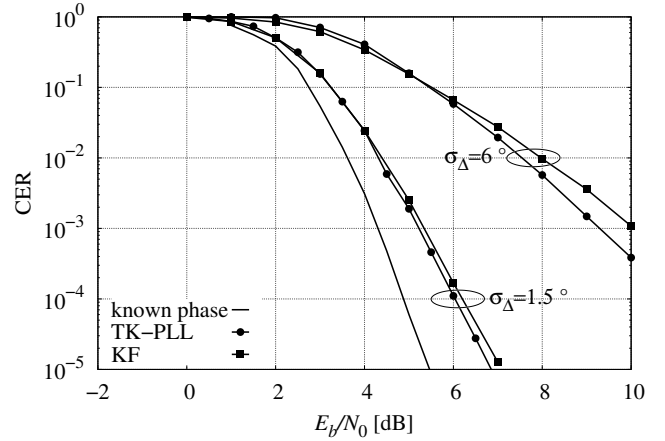


Fig. 7. CER performance of the TK-PLL and the KF schemes for a PN characterized by a  $\sigma_{\Delta}$  of 1.5 and 6 deg.

when  $\sigma_{\Delta} = 1.5$  deg. However, as the PN standard deviation increases, the behavior of  $I_0(\cdot)$  and an exponential function gradually start to differ. This can cause the LLRs of the KF to be less precise representations of the true LLRs. Differently, the  $I_0(\cdot)$  function provides a better approximation of the LLRs, which is reflected in the performance improvement observed in Fig. 7. The TK-PLL's performance could be further improved using more advanced algorithmic features such as those in [4], [5], [17] and references therein. For example, in [5] and [17], Tikhonov mixtures of different orders are used to approximate the SPA messages. As shown in [5], these algorithms represent a set of PLLs with a controller determining the number of tracking loops necessary to maintain tracking on all possible trajectories. Similarly, the decision-aided variant of the Tikhonov algorithm, as discussed in [4], can be implemented using a conventional PLL that makes direct decisions on the symbols based on a threshold for selected symbols. Moreover, both the KF and the TK-PLL performance could be improved by utilizing a non-linear model that matches the non-linear observation equation in (1) [10], [19]–[21].

## VI. CONCLUSION

In this letter, we reviewed the KF and first-type PLLs as an instance of the SPA within the FG framework. We then introduced an alternative first-type PLL scheme based on the Tikhonov distribution. We found that the resulting Tikhonov PLL exhibit similar tracking performance compared to the KF, while surpassing classical PLLs. However, in situations where both demodulation and tracking are required, the Tikhonov PLL outperforms the KF, especially for large values of  $\sigma_{\Delta}$ . This advantage derives from the Tikhonov PLL's ability to better model the pdfs associated with phase estimation.

We believe that the Tikhonov PLL scheme is a new addition to the family of PLLs, with interesting open research directions. Further research could involve establishing its equivalency with higher-order PLLs in the presence of N-dimensional pdfs, enabling frequency shift and rate estimation, and expanding the investigation to other pdfs belonging to the exponential family.

## REFERENCES

- [1] G. Colavolpe, "Communications over phase-noise channels: a tutorial review," in *Proc. 6th Advanced Satell. Mobile Syst. Conf. and 12th Intern. Workshop on Signal Proc. for Space Commun. (ASMS&SPSC 2012)*, Baiona, Spain, Sep. 2012.
- [2] F. Kayhan and G. Montorsi, "Constellation design for memoryless phase noise channels," *IEEE Trans. on Wireless Commun.*, vol. 13, no. 5, pp. 2874–2883, Apr. 2014.
- [3] A. Ugolini, A. Piemontese, and T. Eriksson, "Spiral constellations for phase noise channels," *IEEE Trans. Commun.*, vol. 67, no. 11, pp. 7799–7810, Aug. 2019.
- [4] G. Colavolpe, A. Barbieri, and G. Caire, "Algorithms for iterative decoding in the presence of strong phase noise," *IEEE J. Select. Areas Commun.*, vol. 23, no. 9, pp. 1748–1757, Sep. 2005.
- [5] S. Shayovitz and D. Raphaeli, "Message passing algorithms for phase noise tracking using Tikhonov mixtures," *IEEE Trans. Commun.*, vol. 64, no. 1, pp. 387–401, Dec. 2015.
- [6] G. Colavolpe and A. Modenini, "Iterative carrier synchronization in the absence of distributed pilots for low SNR applications," in *International Workshop on Tracking, Telemetry, and Command for Space*, Darmstadt, Germany, 2013.
- [7] J. Vila-Valls, P. Closas, M. Navarro, and C. Fernandez-Prades, "Are PLLs dead? a tutorial on Kalman filter-based techniques for digital carrier synchronization," *IEEE Aerospace and Electronic Systems Magazine*, vol. 32, no. 7, pp. 28–45, Jul. 2017.
- [8] A. Piemontese, G. Colavolpe, and T. Eriksson, "Discrete-time models and performance of phase noise channels," *IEEE Open Journal of the Communications Society*, Apr. 2024.
- [9] F. R. Kschischang, B. J. Frey, and H.-A. Loeliger, "Factor graphs and the sum-product algorithm," *IEEE Trans. Inform. Theory*, vol. 47, pp. 498–519, Feb. 2001.
- [10] B. D. O. Anderson and J. B. Moore, *Optimal Filtering*. Englewood Cliffs, NJ: Prentice-Hall, 1979.
- [11] N. Assimakis and M. Adam, "Kalman filter riccati equation for the prediction, estimation, and smoothing error covariance matrices," *International Scholarly Research Notices*, vol. 2013, 2013.
- [12] F. M. Gardner, *Phaselock techniques*, 3rd ed. Wiley-Interscience, 2005.
- [13] H. Shu, E. P. Simon, and L. Ros, "Third-order Kalman filter: Tuning and steady-state performance," *IEEE Signal Processing Letters*, vol. 20, no. 11, Aug. 2013.
- [14] G. Christiansen, "Modeling of PRML timing loop as a Kalman filter," in *Proc. IEEE Global Telecommun. Conf.*, vol. 2, Nov. 1994, pp. 1157–1161.
- [15] P. Driessen, "DPLL bit synchronizer with rapid acquisition using adaptive Kalman filtering techniques," *IEEE Trans. Commun.*, vol. 42, no. 9, pp. 2673–2675, Sep. 1994.
- [16] C. Forbes, M. Evans, N. Hastings, and B. Peacock, *Statistical distributions*. John Wiley & Sons, 2011.
- [17] G. Colavolpe, E. Conti, A. Piemontese, and A. Vannucci, "The difficult road of expectation propagation towards phase noise detection," in *Proc. IEEE Intern. Conf. Commun.*, Rome, Italy, Jun. 2023.
- [18] CCSDS 230.1-G-3, *TC Synchronization and Channel Coding - Summary of Concept and Rationale*, Oct. 2021. Available at <http://public.ccsds.org/>
- [19] M. L. Psiaki and H. Jung, "Extended kalman filter methods for tracking weak gps signals," in *Proceedings of the 15th International Technical Meeting of the Satellite Division of the Institute of Navigation (ION GPS 2002)*, 2002, pp. 2539–2553.
- [20] E. A. Wan and R. Van Der Merwe, "The unscented kalman filter for nonlinear estimation," in *Proceedings of the IEEE 2000 Adaptive Systems for Signal Processing, Communications, and Control Symposium (Cat. No. 00EX373)*. IEEE, 2000, pp. 153–158.
- [21] C. Fernández-Prades and J. Vilà-Valls, "Bayesian nonlinear filtering using quadrature and cubature rules applied to sensor data fusion for positioning," in *2010 IEEE International Conference on Communications*. IEEE, 2010, pp. 1–5.